Available online at www.sciencedirect.com
ScienceDirect
International Journal of Hydrogen Energy 32 (2007) 4943–4948
International Journal of HYDROGEN ENERGY
www.elsevier.com/locate/ijhydene

A theoretical study of the electronic structure and bonding of the monoclinic phase of Mg_2NiH_4

Paula V. Jasen[a], Estela A. González[a], Graciela Brizuela[a], Oscar A. Nagel[a], Gustavo A. González[b], Alfredo Juan[a,*]

[a]*Departamento de Física, Universidad Nacional del Sur, Av. Alem 1253, Bahía Blanca 8000, Argentina*
[b]*Departamento de Ingeniería Eléctrica, Electrónica y Computadoras, Universidad Nacional del Sur, Av. Alem 1253, Bahía Blanca 8000, Argentina*

Received 15 June 2007; received in revised form 2 August 2007; accepted 9 August 2007
Available online 29 September 2007

Abstract

The electronic properties of the Mg_2NiH_4 monoclinic phase are calculated using a density functional approach calculation. The crystalline parameters and interatomic distances calculated are close to the experimental values within a 3% error. We also evaluate the density of states (DOS) and character of the chemical bonding for the hydrogen's located in their equilibrium positions. While the Ni–Mg interaction is dominant in the pure alloy, in the hydride the hydrogen atoms present a bonding much more developed with Ni than with Mg. The principal bonding interaction is Ni sp–H s. Moreover, a small bonding between Ni d_{eg} and H 1s is observed. Up the Fermi level, the Ni–H interaction is slightly antibonding. The Mg–Ni bonding interactions are weaker in the hydride phase when compared with the pure Mg_2Ni alloy. The present study is potentially useful because the alloys Mg–Ni are good materials for hydrogen storage.

PACS: 71.15 Mb; 71.15−m; 71.22 Lp

Keywords: Hydride; Mg_2NiH_4; DFT; Electronic structure

1. Introduction

Hydrogen storage materials are one of the key steps for the development of a future clean energy system. For a variety of materials, alloying has been used to improve its hydrogen absorption and desorption characteristics [1–5]. Special interest has been focused on $LaNi_5$, Mg_2Ni, FeTi, or closely related alloys that form semiconducting hydride phases such as Mg_2NiH_4, Mg_2CoH_5 and Mg_2FeH_6 [6–8]. However, despite such great effort, the alloying effect still remains unclear. Therefore, an electronic structure study could be useful to shed more light on this problem [9].

Magnesium-based alloy are considered to be the most promising materials for hydrogen storage because of their storage capacity, the abundance of magnesium in the earth's crust and low-cost compared with alternative systems [6]. Of all the magnesium-based alloys, Mg_2Ni is the most remarkable due to its relatively high-capacity and favourable thermodynamics [10,11]. It absorbs hydrogen at moderate temperatures and pressures and forms a hydride, Mg_2NiH_4, which contains 3.6 wt% hydrogen. The hydrogen absorption rate of pure magnesium is greatly improved by alloying with Ni due to the catalytic activity of the transition metal.

Since 1968, when Reilly and Wiswall [12] discovered the reversible hydrogen adsorption ability of the Mg_2Ni to form the ternary hydride Mg_2NiH_4, its physics and chemistry have been a matter of study [1–5,11,13–21]. Most studies have performed experimental research and many works have been dedicated to the high-temperature (HT) phase (CaF_2 type structure) [22,23]. Only a few studies have analysed the electronic structure by quantum chemical calculations [7,9,23–25].

Upon hydrogenation, Mg_2Ni transforms into the hydride phase Mg_2NiH_4, so as to form a stable covalent-type bonding composed of Mg^{2+} and $[NiH_4]^{4-}$ complex [15]. Each Ni atom is surrounded by four hydrogen atoms in a tetrahedral array,

* Corresponding author. Fax: +54 291 4595142.
E-mail address: cajuan@criba.edu.ar (A. Juan).

0360-3199/$ - see front matter © 2007 International Association for Hydrogen Energy. Published by Elsevier Ltd. All rights reserved.
doi:10.1016/j.ijhydene.2007.08.011

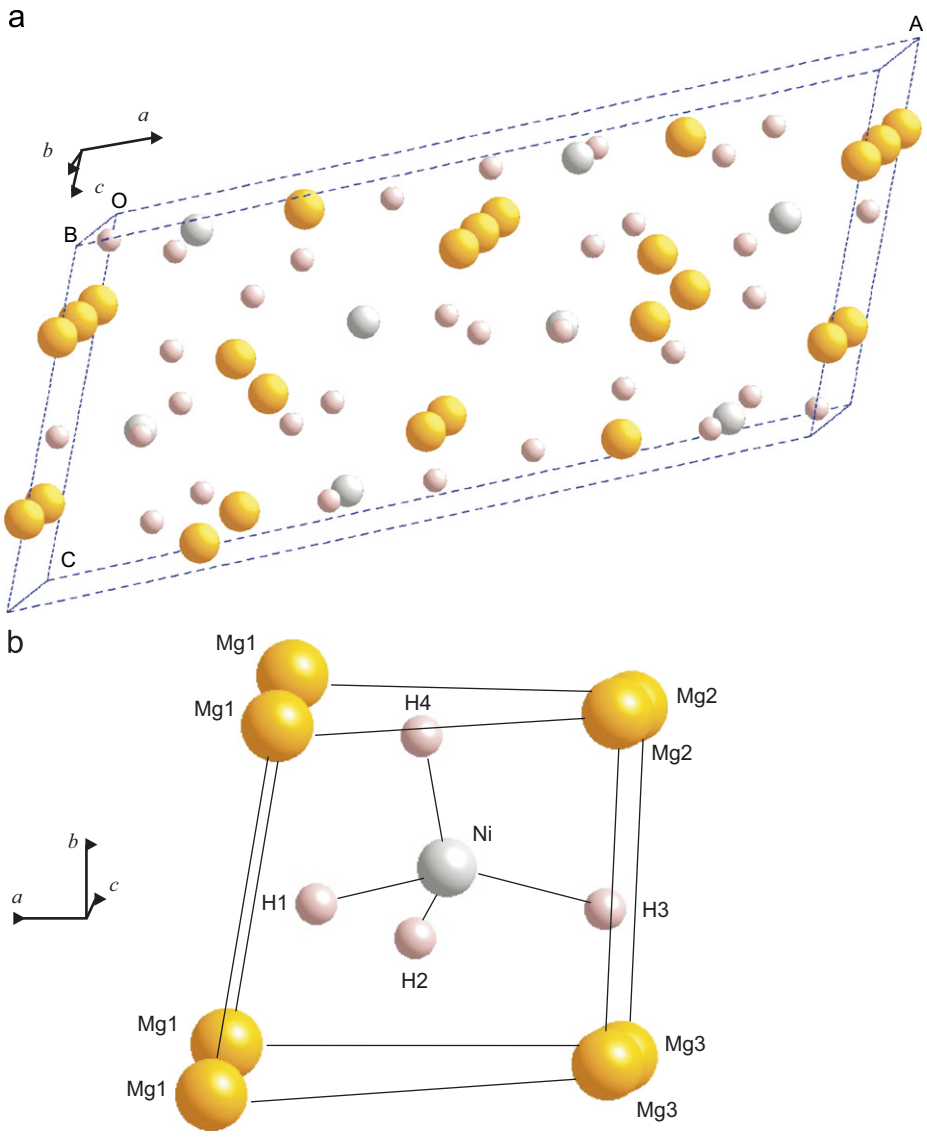

Fig. 1. Schematic view of the unit cell of the Mg_2NiH_4 hydride (a) and minimal representation of the structure (b).

Table 1
Atomic positional parameters in direct coordinates for Mg_2NiH_4 LT phase

Atom	Experimental[a]			Calculated/optimized		
	x	*y*	*z*	*x*	*y*	*z*
H1	0.2113	0.2995	0.3037	0.211	0.300	0.308
H2	0.1360	0.3163	0.8811	0.137	0.315	0.882
H3	0.0105	0.2868	0.5370	0.011	0.287	0.536
H4	0.1306	0.9950	0.0815	0.131	0.994	0.081
Mg1	0.2652	0.4827	0.0754	0.262	0.484	0.074
Mg2	0.0000	0.0144	0.2500	0.000	0.018	0.250
Mg3	0.0000	0.5130	0.2500	0.000	0.516	0.250
Ni	0.1194	0.2308	0.0832	0.119	0.230	0.083

[a]Atomic positions determinate by X-ray diffraction profile at room temperature by Zolliker et al. [30].

with short Ni–H bond lengths and Mg–H bonds slightly longer than those in magnesium hydride (MgH_2) [26].

Below 510 K, Mg_2NiH_4 exhibits a monoclinic distorted low-temperature (LT) modification of a cubic HT phase, where

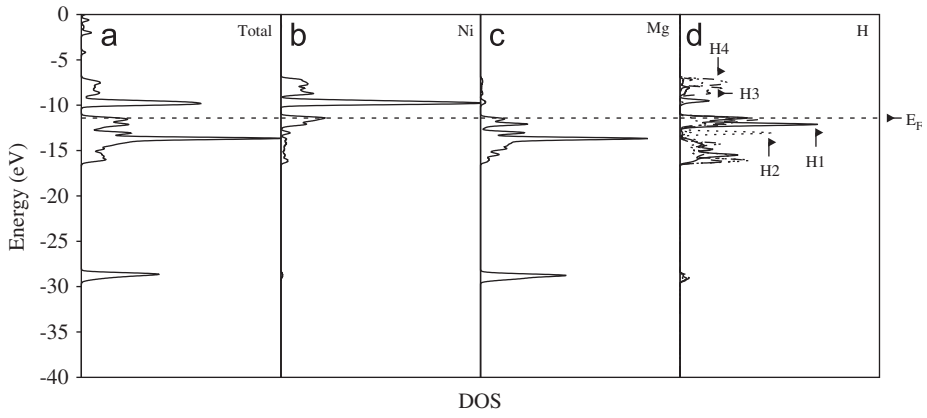

Fig. 2. DOS curves for the Mg_2NiH_4 hydride. Total (a), DOS projected on a Ni atom (b), on a Mg atom (c) and on the four H atom shown in Fig. 1(b).

Table 2
Electron density, overlap population and distances for Mg_2Ni and for Mg_2NiH_4 LT phase

Structure	Electron density			Bond type	OP[a]	Distance (Å)
	s	p	d			
Mg_2Ni						
Ni1	0.15	0.18	3.56	Ni–Ni	0.000	4.41
Ni2	0.13	0.16	4.00	Ni1–Ni2	0.231	2.60
Mg1	1.94	5.84	0.00	Mg–Mg	0.000	2.86
				Ni1–Mg1	0.083	2.70
Mg2	1.95	5.89	0.00	Ni1–Mg2	0.108	2.52
				Ni2–Mg1	0.068	2.70
				Ni2–Mg2	0.107	2.52
Mg_2NiH_4						
Ni	0.35	0.50	1.81	Ni–Ni	0.000	3.92
Mg1	1.94	5.70	0.00	Ni–Mg1	0.084	2.40
Mg2	1.94	5.70	0.00	Ni–Mg2	0.046	2.48
Mg3	1.96	5.77	0.00	Ni–Mg3	0.088	2.74
H1	1.40	0.00	0.00	Ni–H1	0.375	2.05
H2	1.33	0.00	0.00	Ni–H2	0.560	1.50
H3	1.15	0.00	0.00	Ni–H3	0.445	1.61
H4	1.14	0.00	0.00	Ni–H4	0.463	1.52
Mg1	1.94	5.66	0.00	Mg1–H4	0.025	1.84
				Mg1–H3	0.013	1.98

$E_F = -11.42$ eV.
[a]OP: Overlap population.

magnesium ions form a cube around zerovalent NiH_4-complex in an antiflourite arrangement [27]. The orientation of the NiH_4 complex is quenched in a monoclinic distortion of the cubic (CaF_2) HT phase [28]. The phase transformation in Mg_2NiH_4 is essentially due to an order–disorder transition of the hydrogen atoms [11,29]. In the HT phase the hydrogen atoms perform a rapid reorientation motion around the central nickel atom. In the LT phase, this motion is 'frozen' and an ordered arrangement of slightly distorted tetrahedral NiH_4-complex is observed by neutron diffraction [19,29].

Under normal conditions Mg_2NiH_4 is a stable compound, i.e. at room temperature the equilibrium pressure is so low that Mg_2NiH_4 practically does not desorb hydrogen. Therefore, it is essential to decrease the stability of Mg_2NiH_4 to produce a suitable material for practical hydrogen storage [25,27].

Recently, an ab initio total-energy density functional study was used to investigate the LT form of Mg_2NiH_4 [14]. This hydride phase was found to be a semiconductor with a band gap of 1.4 eV.

Häussermann et al. have showed the bonding and stability of hydrogen storage materials Mg_2NiH_4 (LT) and compared with those of Ba_2PdH_4 using DFT calculations. The differences in the bonding between both compounds are originated in the difference strength of the TM–H interactions [30].

We expect to contribute with theoretical calculations to the understanding of bonding in this Mg–Ni hydride.

2. Crystal structure and calculation methods

Zolliker et al. determined the structure of the unit cell for LT phase of Mg_2NiH_4 from a combined study of high-resolution

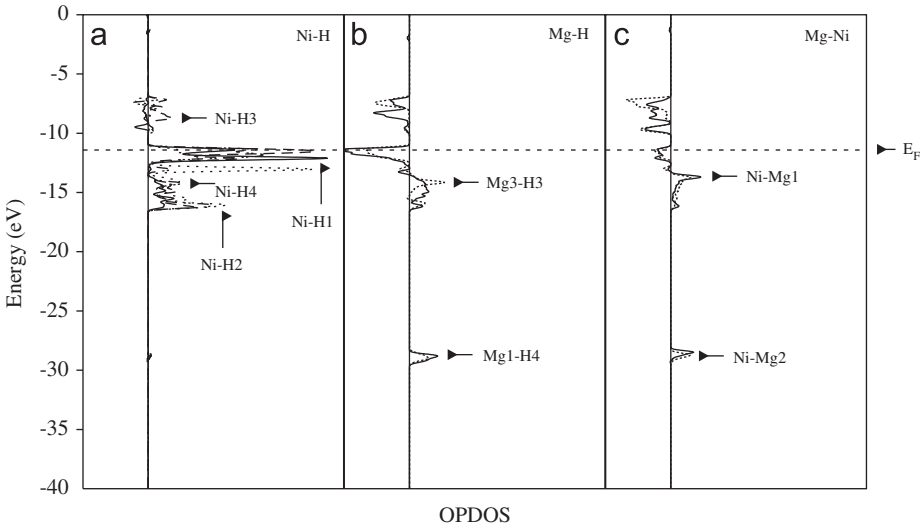

Fig. 3. OPDOS curves for the Mg_2NiH_4 hydride for the Ni–H (a), Mg–H (b) and Mg–Ni (c) bonds.

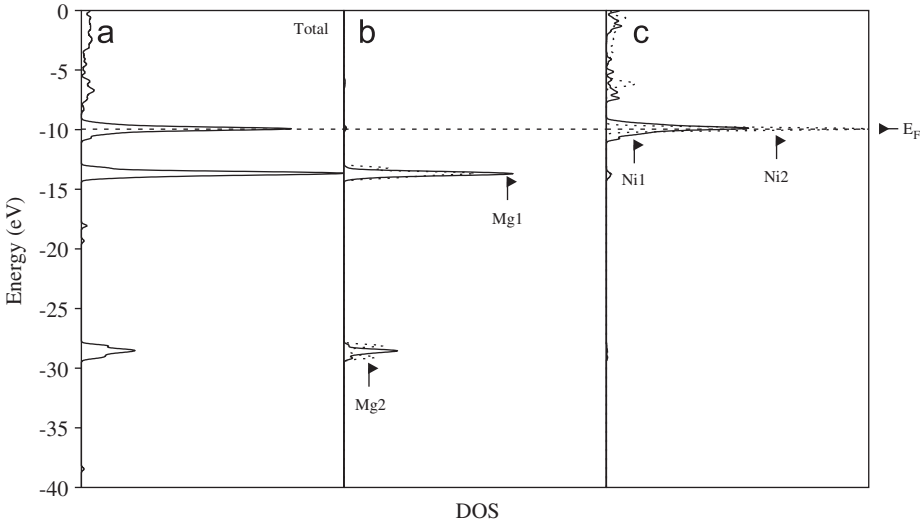

Fig. 4. DOS curves for the Mg_2Ni alloy. Total (a), DOS projected on Ni atoms (b) and on Mg atoms (c) for each type of the metallic atom.

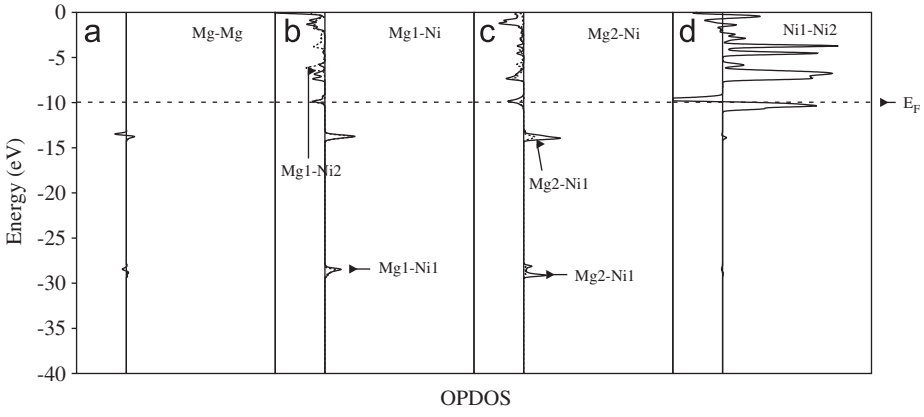

Fig. 5. OPDOS curves for the Mg_2Ni alloy for the Mg–Mg (a), Mg1–Ni (b), Mg_2–Ni (c) and Ni–Ni (d) bonds.

Table 3
Orbital overlap population contribution to the Ni–H and Mg–H bonds

Orbital		Mg%	Ni%								
		2s	4s	$4p_x$	$4p_y$	$4p_z$	$3d_{x^2-y^2}$	$3d_{z^2}$	$3d_{xy}$	$3d_{xz}$	$3d_{yz}$
H1	1s	–	28	13	0.26	64	1.87	2.13	0.26	15.7	2.4
H2	1s	–	30.5	0.36	6.96	33.2	0.53	16.96	0.53	2.14	8.93
H3	1s	–	31	31.2	2.47	0.90	21.12	7.19	4.04	2.25	–
H4	1s	100	34.56	0.21	27.21	–	30.24	7.56	0.21	–	–

X-ray and time-of-flight neutron powder diffraction data [11,31]. It has a monoclinic symmetry (space group C2/*c*) with parameters $a = 14.343$ Å, $b = 6.4038$ Å, $c = 6.4830$ Å (Fig. 1(a)).

The atomic positional parameters in direct coordinates are indicated in Table 1. The H atoms are surrounded by the Ni atoms in a nearly regular tetrahedral configurations. Each H atoms is bonded to one Ni atom and has either four (H2, H3, H4) or three (H1) nearest Mg atom neighbours. Three of the H atoms (H2, H3 and H4) are located near the centres of the face of a (deformed) cube, in such a way that these atoms form nearly tetrahedral angles with the Ni atom. The fourth H atom (H1) is located away from a centre of the face, thereby strongly displacing one of the alkaline metal atoms (Mg1) (Fig. 1(b)).

Gradient-corrected density functional theory (GC-DFT) calculations [32,33] were performed on a Mg–Ni hydride containing 13 atoms in a monoclinic lattice to model bulk Mg_2NiH_4, with a $8 \times 8 \times 8$ reciprocal space grid in the supercell Brillouin zone and a plane wave kinetic energy cutoff of 500 eV for the Mg–Ni–H system [30,32–34]. We use the Amsterdam Density Functional 2000 (ADF-BAND2000) [35]. The molecular orbitals were represented as linear combination of Slater functions. For the gradient correction, the Becke [36] approximation for the exchange energy functional and the Lee et al. [37] approximation for the correlation functional were employed.

In order to increase the computational efficiency, the internal atomic layers are kept frozen for every atom except hydrogen, since the internal electrons do not contribute significantly to the bonding. A basis set of triple-ζ quality was used (this means three Slater-type functions for each atomic valence orbital occupied) with polarization functions to express the atomic orbitals of Mg and Ni. The basis set of Ni consisted of 3d, 4s and 4p orbitals and for Mg 2s and 2p. To understand the Mg–Ni–H system interactions, we used the concept of density of states (DOS) and overlap population density of states (OPDOS). The DOS curve is a plot of the number of orbitals as a function of the energy. The integral of the DOS curve over an energy interval gives the number of one-electron state in that interval; the integral up to the Fermi level (E_F) gives the total number of occupied molecular orbitals. If the DOS is weighted with the overlap population between two atoms the OPDOS is obtained. The integrations of the OPDOS curve up to E_F gives the total overlap population of the specific bond orbital and it is a measure of the bond strength. If an orbital at certain energy is strongly bonding between two atoms, the overlap population is strongly positive and OPDOS curve will be large and positive around that energy. Similarly, OPDOS negative around certain energy corresponds to antibonding interactions.

The absorption energy was computed as the difference ΔE between the Mg–Ni–H composite system when the H atom is absorbed at its minima location geometry and when it is far away from the Mg–Ni alloy.

3. Results and discussion

We started our calculations considering the stability of the alloy and the hydride formation. The Mg_2NiH_4 LT phase is 1.37 eV more stable than Mg_2Ni plus two hydrogen molecules. This value is in good agreement with that of Häussermann et al. [30].

In Fig. 2 we have plotted the total DOS for the Mg_2NiH_4 LT phase hydride and the projected DOS on Ni, Mg and H atoms in its optimum geometry. The band at −28 eV comes from Mg p based states somewhat mixed with H based states. The contribution of Ni to this band is very small. The metal Ni d states form a main band between −17 and −11 eV. Mg presents a band in the same region and is composed by s and p states. H states are mainly located close to the Ni states.

The states above the Fermi level correspond to Ni d_{tg} and H states (see the sharp peak near −10 eV). The band gap above E_F is 1.5 eV, which is close to that reported by Richardson et al. [26] and Häussermann et al. [30]. The band gap of Mg_2NiH_4 has been determined experimentally by Lupu et al. [38] with a value of 1.68 eV. The DOS is similar to that reported by Myers et al. [14] and Häussermann et al. [30].

Table 2 summarizes the distances, electronic density and overlap populations for selected bonds. It can be seen that the Ni–H interaction present the higher OP, the Ni–Mg bond is small. There is also a small Mg–H bond. The Ni–Ni bond in the pure alloy is 0.231 while the Ni–Mg OP is 0.070–0.110. The first interaction not present in the hydride phase and the second one is reduced to its half value in the case of Mg_2. The Ni–H distances are close to that reported by Häussermann et al. (1.516 Å) while the Mg–H distances are a little bit shorter (1.9 Å vs. more 2.0 Å from [30]).

The OPDOS curves in Fig. 3 shows that the Ni–H interaction between −11 and −18 eV are bonding and the Ni–Ni is non-bonding. The Ni–Mg and Mg–H OPDOS both have antibonding states near the E_F.

The DOS of the Mg_2Ni alloy is shown in Fig. 4 and the OPDOS curves for Mg–Mg, Mg–Ni and Ni–Ni are shown in Fig. 5. The more important interaction in the alloy is Ni1–Ni2

(see Fig. 5(d)). The Ni–Ni bond in the hydride phase is not present because four hydrogen atoms surround each Ni.

The compositions of each atomic orbital to the Ni–H and Mg–H bonds are shown in Table 3. The main interactions are Ni 4s–H 1s. In the case of H1 and H2 there is also an important contributions coming from Ni $4p_z$ orbitals and in the case of H3 and H4 from Ni $4p_y$ and $3d_{x^2-y^2}$. The Mg–H interaction is only developed through the 2s–1s orbitals (see Table 3). There is no H–H interaction present. Our results confirm the hydride behaviour of Mg_2NiH_4 (LT) that is partially as an ionic hydride. $Mg^{2+}H_2^-$ and partially are hydride complex $Mg_2^{2+}Ni^0H_4^{4-}$.

4. Conclusion

We calculated the electronic structure and bonding of the LT phase of Mg–Ni hydride. Our calculations are in good agreement with previous reports and also reveal that the main bonding interaction comes from Ni sp–H s orbitals and s orbitals in the case of Mg. The computed Ni–H distances are close to that previously reported while the Mg–H distances are a little bit shorter. The Mg_2–Ni bonds decrease its strength to half the value when compared with the pure alloy. No Ni–Ni bonds are detected in the hydride phase.

Acknowledgements

SEGCyT-Física-UNS, CONICET, J.S. Guggenheim Foundation, CIC-Bs. As. and Fulbright Commission supported our work. A. Juan and G. Brizuela are members of CONICET, E. Gonzalez and P. Jasen are fellows of that Institution.

References

[1] Goren SD, Korn C, Mintz MH, Gavra Z, Hadari Z. J Chem Phys 1980;73:4758.
[2] Blomqvist H, Rönnebro E, Noréus D, Kuji T. J Alloys Compd 2002;330–332:268.
[3] Fujii H, Orimo S, Ikeda K. J Alloys Compd 1997;253–254:80.
[4] Orimo S, Fujii H. Intermetallics 1998;6:185.
[5] Tessier P, Akiba E. J Alloys Compd 2000;302:215.
[6] Noréus D, Olson LG. J Chem Phys 1983;78:2419.
[7] Linderberg P, Noréus D, Blomberg MRA, Siegbahn PEM. J Chem Phys 1986;85:4530.
[8] Buchner H. International symposium on hydrogen for energy storage. Geilo, Norway; 1977.
[9] Yukawa H, Matsumura T, Morinaga M. J Alloys Compd 1999; 293–295:227.
[10] Grava Z, Mintz MH, Kimmel G, Hadari Z. Inorg Chem 1979;18:3595.
[11] Zolliker P, Yvon K, Jorgensen JD, Rotella F. Inorg Chem 1986;25:3590.
[12] Reilly JJ, Wiswall Jr RH. Inorg Chem 1968;7:2254.
[13] Gavra Z, Kimmel G, Gefen Y, Mintz MH. J Appl Phys 1985;57:4548.
[14] Myers WR, Wang L-W, Richardson TJ, Rubin MD. J Appl Phys 2002;91:4879.
[15] Orimo S, Zúttel A, Ikeda K, Saruki S, Fukunaga T, Fujii H, Schlapbach L. J Alloys Compd 1999;293-295:437.
[16] Orimo S, Fujii H. Intermetallics 1998;6:185.
[17] Zeng K, Klassen T, Oelerich W, Bormann R. J Alloys Compd 1999;283:213.
[18] Yamamoto S, Fukai Y, Rönnebro E, Chen J, Sakai T. J Alloys Compd 2003;356–357:697.
[19] Enache S, Lohstroh W, Griessen R. Phys Rev B 2004;69:115326.
[20] Mohamad AA, Alias Y, Arof AK. J New Mater Electrochem Syst 2003;6:205.
[21] Blomqvist H, Noréus D. J Appl Phys 2002;91:5141.
[22] Yvon K, Shefer J, Stucki F. Inorg Chem 1981;20:2776.
[23] García GN, Abriata J, Sofo JO. Phys Rev B 1999;59:11746.
[24] García GN, Abriata J, Sofo JO. Phys Rev B 2002;65:064306.
[25] Takahashi Y, Yukawa H, Morinaga M. J Alloys Compd 1996;242:98.
[26] Richardson TJ, Slack JL, Armitage RD, Kostecki R, Farangis B, Rubin MD. Appl Phys Lett 2001;78:3047.
[27] Blomqvist H, Rönnebro E, Noréus D, Kuji T. J Alloys Compd 2002;330–332:268.
[28] Guthrie SE, Thomas GJ, Noréus D, Rönnebro E. Mater Res Soc Symp Proc 1998;513:93.
[29] Zolliker P, Yvon K, Baerlocher CH. J Less-Common Met 1986;115:65.
[30] Häussermann U, Blomqvist H, Noréus D. Inorg Chem 2002;41:3684 and references therein.
[31] Zolliker P, Yvon K, Baerlocher Ch, Jorgensen JD, Rotella F. J Less-Common Met 1987;129:208.
[32] Hohenberg P, Kohn W. Phys Rev B 1964;136:864.
[33] Kong W, Sham LJ. Phys Rev B 1965;140:1133.
[34] Parr RG, Yang W. Density functional theory of atoms and molecules. New York: Oxford University Press; 1989.
[35] Amsterdam Density Functional Package Release 2001. Vrije Universiteit, Amsterdam.
[36] Becke D. Phys Rev A 1988;38:3098.
[37] Lee C, Yang W, Parr RG. Phys Rev B 1988;37:785.
[38] Lupu D, Sârbu R, Biris A. Int J Hydrogen Energy 1987;12:425.